Annealing induced photosensitivity modulation of zinc selenide thin film in the sub-band gap optical absorption region

B. Karim, and P. Chottopadhyay

Citation: Journal of Applied Physics **123**, 245701 (2018); doi: 10.1063/1.5029525
View online: https://doi.org/10.1063/1.5029525
View Table of Contents: http://aip.scitation.org/toc/jap/123/24
Published by the American Institute of Physics

Annealing induced photosensitivity modulation of zinc selenide thin film in the sub-band gap optical absorption region

B. Karim and P. Chottopadhyay[a)]
Department of Electronic Science, University of Calcutta, 92 A.P.C. Road, Kolkata 700009, India

(Received 15 March 2018; accepted 3 June 2018; published online 22 June 2018)

The photosensitivity of the chemical bath deposited zinc selenide (ZnSe) thin film of bandgap 2.8 eV air annealed at different temperatures has been studied under sub-band gap optical illuminations of photon energies 1.77, 1.91, and 2.07 eV, respectively. The study reveals significant and systematic changes in the photocurrent even when the photon energy is restricted well below the band gap energy of the material. In addition, the photocurrent decreases more or less exponentially with the annealing temperature, although the absorption coefficients of the annealed samples in the sub-band gap region are seen to be enhanced compared to the as-deposited sample. The XRD measurements show the cubic phase of ZnSe, accompanying additionally the orthorhombic $ZnSeO_3$ crystallites in the deposited film. The study further reveals comparatively stronger crystalline improvement of the $ZnSeO_3$ crystals than the cubic ZnSe crystals upon annealing. The observed photosensitivity of the film is compared to that of the cadmium sulphide film deposited by a chemical bath deposition technique and found to be sharply contrasting in behavior. We attribute the unusual photosensitivity of the ZnSe film to $ZnSeO_3$ crystallites which act simultaneously as self generators and absorbers of photoelectrons in the ZnSe crystals, without effectively contributing to the overall photoconductivity of the material. *Published by AIP Publishing.*
https://doi.org/10.1063/1.5029525

I. INTRODUCTION

The study of zinc selenide (ZnSe), either in the crystalline or in the polycrystalline form, has remained an active field of solid state research due to its widespread application in the area of photonic devices, which includes semiconductor lasers,[1,2] LEDs,[3] photovoltaic cells,[4] and different optical detectors including VIS-blue-UV photodetectors.[5,6] Different workers have processed this material by applying different deposition methods and studied the optoelectronic properties of the material, primarily concentrating on the band-to-band transition region relevant to photonic applications. However, despite prolonged research on the optoelectronic properties of the material, the sub-band gap optical absorption region governed by the defects capable of absorbing photons with energy less than the band gap of the material has been ignored in the majority of the publications. This is particularly important when the material is grown in the polycrystalline form. The recent studies on the polycrystalline sulfide semiconductors have revealed interesting results which indicate sub-band gap electronic excitations from the deep levels and the localized states at the grain boundaries of the material.[7] The electronic transitions eventually lead to the sub-band gap absorption tail, known to be largely influenced as a result of annealing. In spite of several reports on the occurrence of sub-band gap absorption, the photoconductivity of the polycrystalline ZnSe film in the said absorption region is still not adequately studied. We have undertaken this particular issue and studied the photoconductivity of the chemically bath deposited ZnSe thin films in the sub-band gap optical absorption region. The results of the investigations are reported in this communication.

[a)]Author to whom correspondence should be addressed: pcelc@caluniv.ac.in

II. EXPERIMENTAL

The zinc selenide thin films are deposited on glass substrates by applying the chemical bath deposition technique reported by Bakiyaraj and Dhanasekaran.[8] One of the substrates containing the deposited film is cut into several pieces of which a few are chosen and given an open air heat treatment at 50, 100, 150, and 200 °C, respectively, for a period of 30 min. The thickness of the film as determined by a field effect scanning electron microscope is found to be nearly 2 μm. The ohmic contacts on the samples are established by indium, deposited onto the film by vacuum evaporation. A two probe method is applied to measure the current-voltage characteristics of the samples at room temperature under different sub-band gap optical illuminations of intensities 2700, 9800, and 13 900 Lux and the photon energies 1.77, 1.91, and 2.07 eV, respectively. At the time of I-V measurements, we have found considerable current instability at low voltages. This we apprehend to be due to highly resistive and polycrystalline nature of the sample. To avoid this problem, we measured the current at relatively higher voltages by varying the voltage in steps of 0.3 V. Also in order to avoid the transient effects observed in polycrystalline ZnSe films,[9–12] we have given sufficiently long time for the stabilization of the sample current. The optical absorption spectra of the samples are measured using a UV-VIS spectrophotometer, followed by XRD measurements to determine the crystal structure of the deposited film. The energy dispersive spectroscopy (EDS) measurements are made to determine the composition of the films.

III. RESULTS AND DISCUSSION

The current density vs. electric field characteristics of the as-deposited and annealed ZnSe thin films are shown in

Figs. 1(a) and 1(b), respectively. The characteristics for both the samples show distinct photosensitivity even for photon energy less than the band gap energy of the material. To get a more clear view of the sub-band gap photosensitivity of the material, we have determined the photocurrent of the samples by subtracting the dark current from the total measured current in the sub-band gap absorption region. The photocurrent density vs. electric field plot for different sub-band gap photon energies is shown in the inset of Figs. 1(a) and 1(b) for the as-deposited sample and the sample annealed at 200 °C, respectively. In both the cases, the photocurrent density varies more or less linearly with the electric field and changes systematically as a result of the combined effect of the photon flux and the photon energy restricted below the band gap energy of the material. What seems to be interesting to note from Fig. 2 that the decrease in the photocurrent is nearly exponential with the annealing temperature and may be fitted by the relation

$$I_{Ph} = I_0 \exp(-\eta T_A), \tag{1}$$

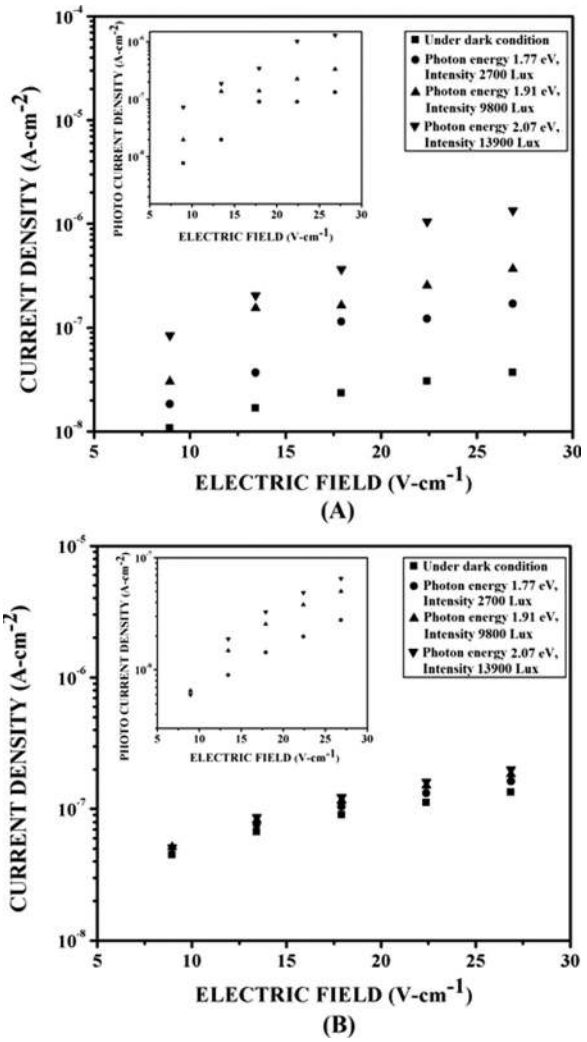

FIG. 1. The current density vs. electric field characteristics of as-deposited (a) and 2000 °C annealed (b) ZnSe thin films under sub-band gap optical illumination. The insets in (a) and (b) show the variations of the photocurrent density with electric field for as-deposited and annealed ZnSe samples under sub-band gap optical illumination.

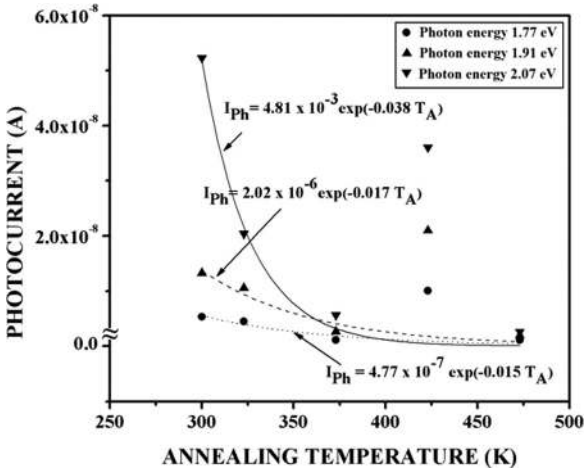

FIG. 2. The variation of photocurrent of the ZnSe thin film with annealing temperature for different sub-band gap photon energies.

where T_A is the annealing temperature and I_0 and η are fitting parameters. The parameter I_0 varies from 4.77×10^{-7} A to 4.81×10^{-3} A as the photon energy increases from 1.77 eV to 2.07 eV. Over the same range of photon energy, the parameter η varies from $-0.015\,K^{-1}$ to $-0.038\,K^{-1}$. A large scattering of data corresponding to the 150 °C annealed sample constrained us to include them in obtaining the fitted relation. In order to examine the significance of the results, we have plotted in Fig. 3 the photocurrent as a function of inverse annealing temperature. As may be seen from the figure, the nature of variation of the photocurrent is not strictly Arrhenius. The variation, however, indicates a possible correlation of the parameter η with the activation energy and the pre-factor I_0 to be implicitly related to the defects in the film.

The effect of annealing is further reflected from the plot of sample resistance as a function of photon energy for the as-deposited sample and the sample annealed at 200 °C shown in Fig. 4. The variation of the resistance is found to be much sharper for the as-deposited sample compared to the annealed one and can be fitted linearly, with slopes and intercepts, $1.04 \times 10^9\,\Omega\,(eV)^{-1}$ and $2.17 \times 10^9\,\Omega$, respectively, for the

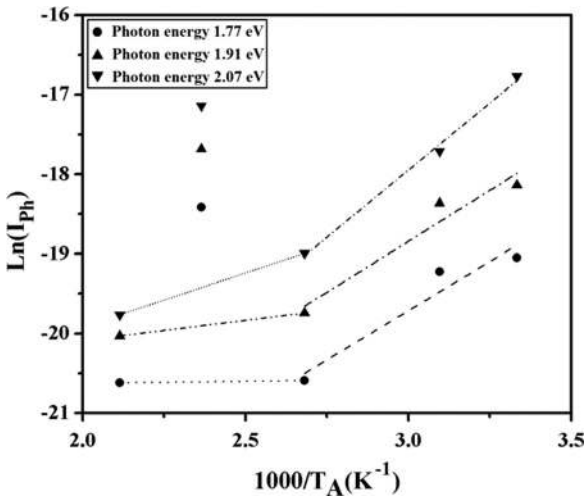

FIG. 3. The logarithmic variation of the photocurrent of ZnSe thin film with the inverse annealing temperature.

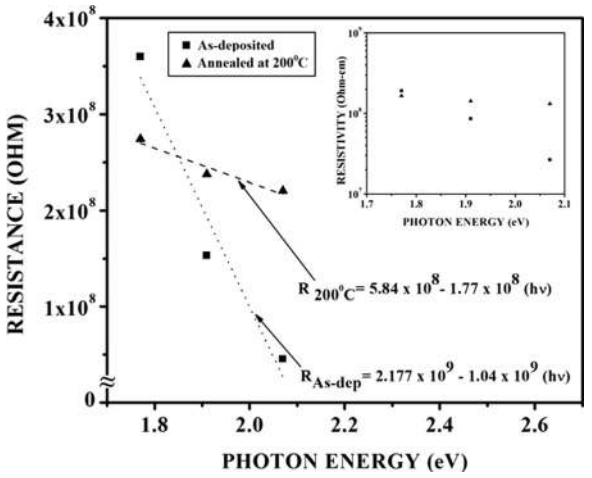

FIG. 4. The variation of resistance of ZnSe thin film with the photon energy for the as-deposited sample and the sample annealed at 200 °C. The inset shows the variation of the resistivity of the material with the photon energy.

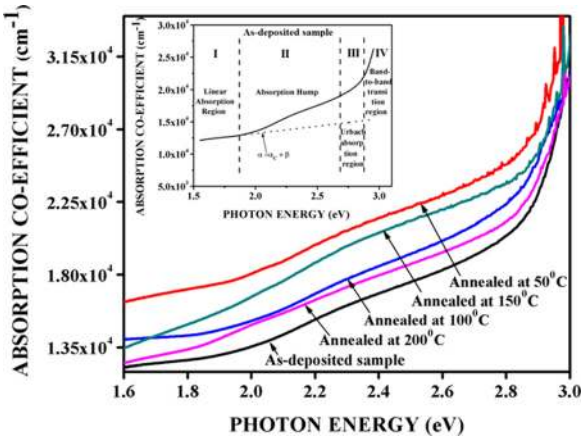

FIG. 5. The variation of the optical absorption co-efficient of the as-deposited and annealed ZnSe thin films. The inset shows the four different optical absorption regions for the as-deposited sample.

as-deposited sample and $1.77 \times 10^8\ \Omega\ (\mathrm{eV})^{-1}$ and $5.84 \times 10^8\ \Omega$, respectively, for the 200 °C annealed sample. For further analysis of the results, we have estimated from the J-E plots, the resistivities of the samples. The variation of the resistivity as a function of photon energy with annealing temperature as the parameter is shown in the inset of Fig. 4. The plot clearly shows the significance of sub-band gap photon energy and annealing on the sample resistivity.

The observed photoconductivity in the sub-band gap photo absorption region cannot be accounted for applying the well known Petritz's model[13] as the model applies to the band-to-band absorption region and neglects space charge density in the grains constituting the polycrystalline material. Rakhshani[14] has considered excess carrier concentration due to the absorption of photons and a change in the carrier mobility, assuming a single defect level instead of distributed defects at the grain boundaries of the material. It is, however, possible that these distributed defects at the grain boundaries coupled with discrete energy levels such as deep levels can play a vital role in controlling the sub-band gap photoconductivity of the sample. It has been pointed out earlier that the above defects play crucial role in the sub-band gap optical absorption in the polycrystalline CdS thin film.[7] Therefore, to explore the origin of excess photoconductivity of the film, the sub-band gap optical absorption spectra of the as-deposited and annealed films are critically analyzed. The absorption curves in Fig. 5 show a sharp rise near the absorption edge due to band-to-band transitions accompanying an elongated absorption tail in the sub-band gap region. However, a closer view revealed an absorption hump in the intermediate range of photon energies which eventfully allows one to decompose the whole absorption curve into four regions, namely, a constant region, the absorption hump, the Urbach region, and the band-to-band transition region. For illustration, the four regions of the absorption model are shown separately in the inset for the as-deposited sample. The observation is in contrast to the chemical bath deposited (CBD) deposited CdS thin film where the absorption curve has been described by three absorption regions.[7] Moreover, the absorption spectra in the sub-band gap region indicate its sensitivity to the annealing temperature, thereby reflecting the apparent enhancement in the absorption co-efficient of the samples. We have estimated the Urbach energy for each of the absorption curves of the ZnSe samples by applying the Urbach exponential law[15] and found the Urbach energy to be varying from 1.87 eV for the as-prepared sample to 2.2 eV corresponding to the sample given heat treatment at 200 °C. The subsequent analyses of the data in the region I suggest a linear law, may be described by the relation $\alpha = \alpha_c + \beta\ (h\nu)$, where α_c and β are the fitting parameters. The parameters are found to be sensitive to the annealing temperature. For instance, the values of α_c and β vary from $8608\ \mathrm{cm}^{-1}$ and $2289\ \mathrm{cm}^{-1}\mathrm{eV}^{-1}$ for the as-deposited sample to $4217\ \mathrm{cm}^{-1}$ and $5786\ \mathrm{cm}^{-1}\mathrm{eV}^{-1}$ for the sample annealed at 200 °C. While the linear variation indicates excitations from the deep levels, the absorption hump next to this linear region is somewhat complex. To get an intuitive idea of the possible factors causing the absorption hump, we carefully investigated the compositional and structural properties of the ZnSe thin film under as-deposited and annealed conditions. Figure 6 shows the EDS results for all the samples. The analysis of the results confirms the presence of Zn, Se, and O in all samples, though no appreciable deviation in their contents is noticed upon annealing. The atomic percentage of Zn remains almost invariant in the annealed samples, whereas the percentages of Se and O fluctuate a bit in the annealed samples compared to the as-prepared one. Besides, no additional impurity element has been identified in the EDS graphs of the samples, before or after annealing, except for an insignificant trace of sodium in the as-deposited sample. In view of this observation, it is unlikely that the variation in the composition upon annealing has played any distinctive role in the sub-band gap absorption hump. More likely, the absorption hump has emerged due to the presence of an additional defect or mixed phase comprising ZnSe nano-crystals and other crystalline phases. The XRD patterns shown in Fig. 7 clearly indicate the presence of a cubic phase of ZnSe (JCPDS 80-0021) accompanying the orthorhombic phase of $ZnSeO_3$ crystals (JCPDS 78-0446). In a number of studies, the presence of $ZnSeO_3$ crystallites in

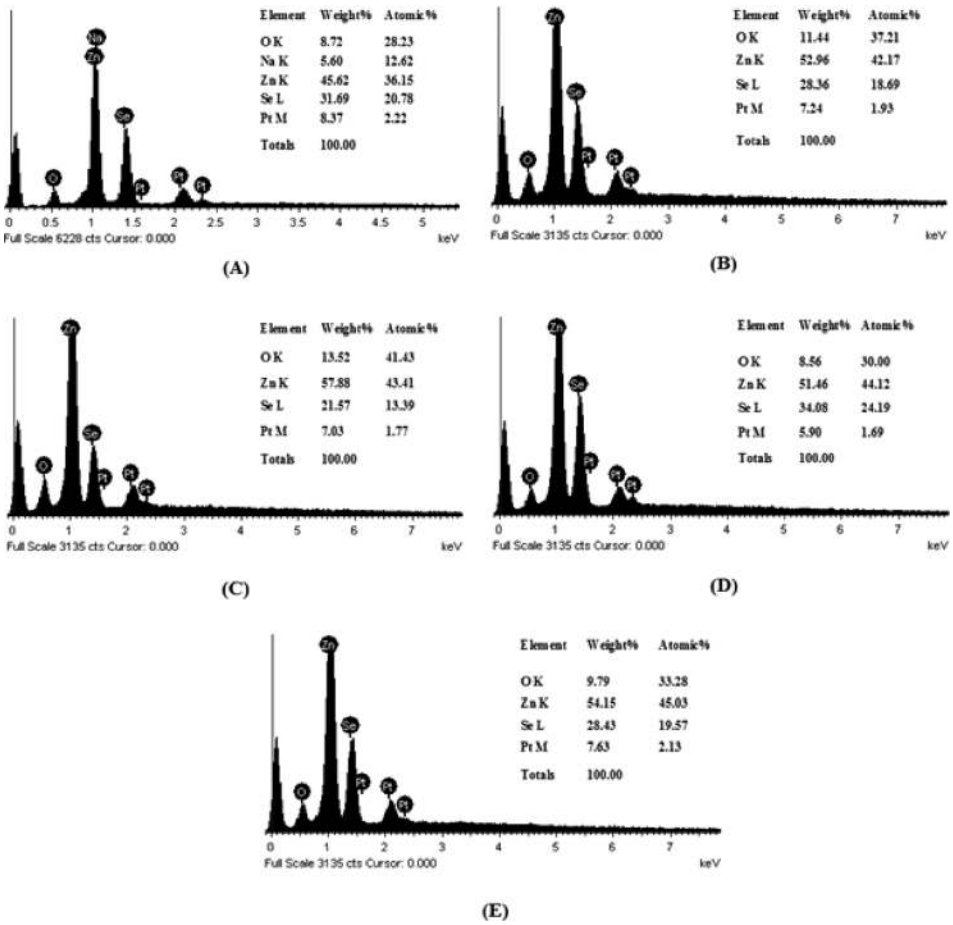

FIG. 6. The EDS graphs for the as-deposited and annealed ZnSe samples. (a) As-deposited, (b) annealed at 50 °C, (c) annealed at 100 °C, (d) annealed at 150 °C, and (e) annealed at 200 °C.

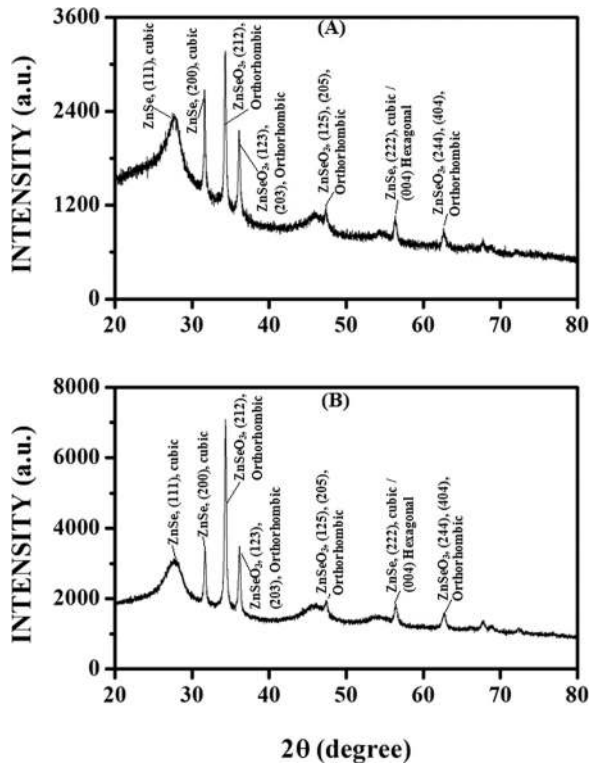

FIG. 7. The XRD pattern of the ZnSe thin film deposited by the chemical bath deposition technique. (a) As-deposited sample and (b) sample annealed at 200 °C.

ZnSe films has been reported.[16–18] The present results further confirm the occurrence of $ZnSeO_3$ crystallites in the CBD ZnSe thin film. Interestingly, compared to the as-deposited sample, the XRD peak intensity is found to be increased substantially for the annealed samples, thereby indicating an improved crystallinity of the $ZnSeO_3$ phase. We have further considered the possibility of $ZnSeO_3$ formation after annealing. However, the formation of $ZnSeO_3$ is very unlikely as the ZnSe samples are annealed at 200 °C or below in the present study. The occurrence of $ZnSeO_3$ has been reported relatively at higher temperature, e.g., annealing at 623 K and above for 24–26 h.[19,20] Verma *et al.*[21] reported the formation temperature of $ZnSeO_3$ to be 442 °C. There are several other reports where $ZnSeO_3$ has been found to be absent even at an annealing temperature of 500 °C and above[22,23] or present in insignificant amounts after annealing in the temperature range of 430–700 °C.[24] Therefore, the growth of $ZnSeO_3$ is unlikely for the annealing temperature restricted at 200 °C or below in the present work. Moreover, the EDS results do not show any definite and significant increase in the oxygen content after annealing the material up to 200 °C. Our literature survey on XPS results further reveals the absence of the $ZnSeO_3$ phase at low temperature annealing.[25,26] Therefore, one cannot proceed with gradual segregation of ZnSe into the $ZnSeO_3$ phase with annealing temperature and correlate the enhanced absorption and decreasing conductivity in terms of different bandgaps of the material. Even if, one considers a

layer of $ZnSeO_3$ (bandgap 3.228 eV) on the top of the ZnSe film of bandgap 2.8 eV, the photons should pass through these materials without causing any absorption due to band-to-band electronic transitions, as the photon energy is less than the bandgap energy. An alternative possibility is the absorption of photons as a result of transitions from the defect states in the band gap of the material. Since the XRD measurements confirmed the inherent presence of $ZnSeO_3$ crystals in the as-grown sample and their crystalline character is improved upon annealing, we conclude that these crystallites are simultaneously acting as entities capable of trapping photoelectrons generated in the ZnSe crystals and self photo-carrier generators without contributing much to the overall photoconductivity of the sample. The photo-carrier generation and absorption properties of $ZnSeO_3$ are consistent with the contrasting observation of enhanced optical absorption and reduced photoconductivity upon annealing.

In order to identify further the significance of $ZnSeO_3$ crystals in the ZnSe film, we have compared the photosensitivity of CdS (bandgap 2.42 eV) thin films (chosen as a model semiconductor) grown by the chemical bath deposition technique. The variation of the current density and the photocurrent density of the material with electric field for the same set of sub-band gap optical illuminations is shown in Fig. 8. In this case, the measured photosensitivity is found to be more pronounced for both the as-deposited sample and the sample annealed at 200 °C compared to the ZnSe samples. The values of the resistance as obtained from the current-voltage measurements are plotted as a function of photon energy in Fig. 9 and found to be linear with slopes varying from 1.88×10^7 to 5.4×10^4 $\Omega(\text{eV})^{-1}$ and the intercepts varying from 4.48×10^7 to 2.1×10^5 Ω, respectively, for the as-deposited and annealed samples. As may be seen from the figure, the resistivity of the sample also follows a similar nature of variation. A comparison of the above results with those of ZnSe samples reveals a contrasting impact of annealing on the resistance or the resistivity of the two materials. While the resistance of the CdS thin film decreases upon annealing, the same is found to increase in the case of ZnSe samples. This is further reflected from the variation of photocurrent of the CdS thin film as a function of annealing temperature shown in Fig. 10 for different sub-band gap energies. It is seen that, in contrast to features exhibited by the ZnSe films, the photocurrent increases exponentially with the annealing temperature, which can be fitted by the relation $I_{Ph} = I_0 \exp(\eta T_A)$. In this case, the value of I_0 is found to vary from 9.01×10^{-12} to 1.73×10^{-10} A, while the parameter η varies from $0.027\,K^{-1}$ to $0.022\,K^{-1}$ as the photon energy is increased from 1.77 eV to 2.07 eV. One can possibly associate a layer of CdO (bandgap 2.3 eV) formed due to the heat treatment[27,28] to account for the change in the photocurrent. However, it is reported that such a layer can enhance the dark conductivity of the CdS film, but the overall photoconductivity of the material decreases significantly for the film annealed at 350 °C compared to the samples annealed relatively at lower temperatures.[28] This implies the role of CdO in modulating the photoconductivity of the CdS film to be insignificant in the present case, as the heat treatment was restricted at or below 200 °C. Moreover, as the

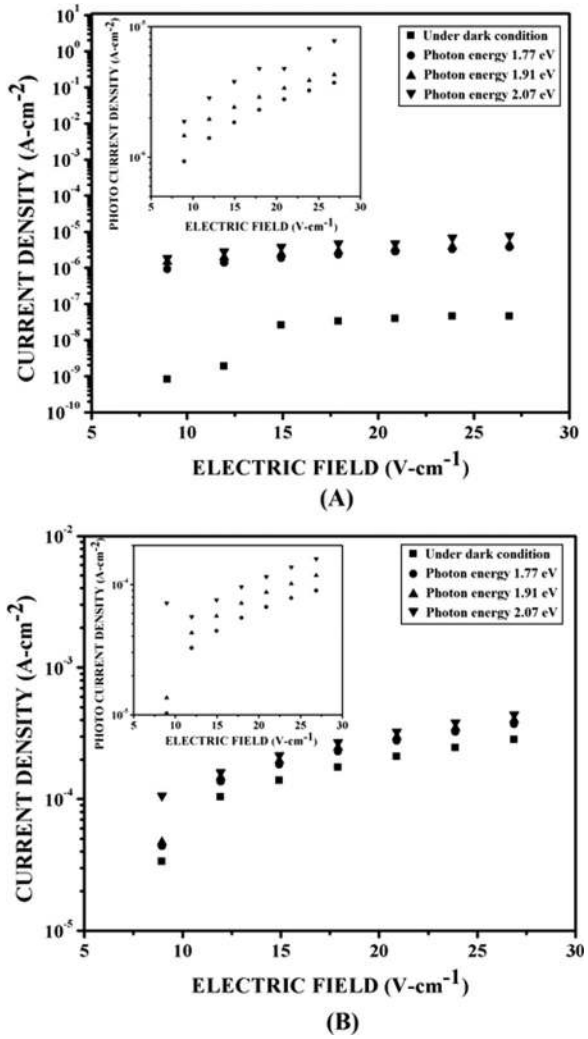

FIG. 8. The current density vs. electric field characteristics of as-deposited (a) and 200 °C annealed (b) CdS thin films under sub-band gap optical illumination. The insets in (a) and (b) show the variations of the photocurrent density with electric field for as-deposited and annealed CdS samples under sub-band gap optical illumination.

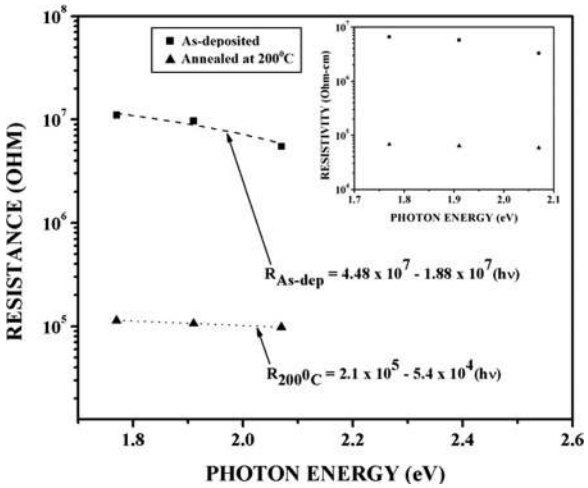

FIG. 9. The variation of resistance of the CdS thin film with the photon energy for the as-deposited sample and the sample annealed at 200 °C. The inset shows the variation of the resistivity of the material with the photon energy.

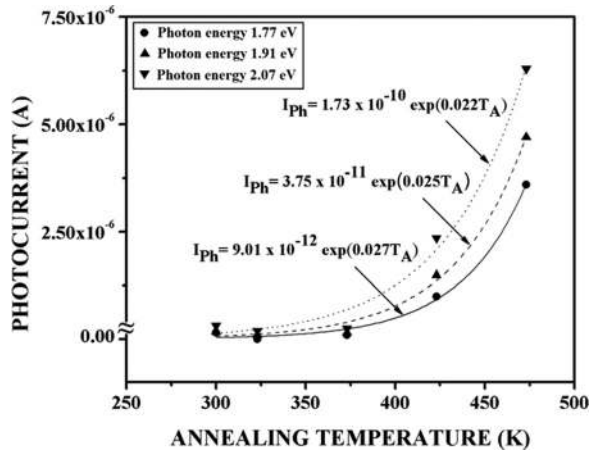

FIG. 10. The variation of the photocurrent of the CdS thin film with annealing temperature for different sub-band gap optical energies.

photon energy is less than the bandgap energies of CdS and CdO, one cannot expect band-to-band excitations. The enhancement of photosensitivity of the CBD CdS thin film may be attributed to the increase in the mobility-lifetime product of free carriers.[29–32] However, the same analogy seems to be inapplicable in the present case of ZnSe thin films. We apprehend that the gradual exponential decay in the photocurrent of ZnSe upon annealing is associated with the grain boundary parameters of the material. Furthermore, the presence of the absorption hump in the absorption spectra of ZnSe films and the absence of the same in the absorption spectra of CBD CdS films studied earlier[7] conclusively prove a definite role of $ZnSeO_3$ in the absorption process compared to the CdS sample.

IV. CONCLUSION

In conclusion, we have studied the sub-band gap photosensitivity of the chemical bath deposited ZnSe thin film for as-deposited and annealed conditions. The photocurrent density in all samples varies systematically even when the photon energy is below the band gap energy of the material. Interestingly, the photosensitivity of the material is seen to decay almost exponentially with the annealing temperature. The results further reveal that the presence of $ZnSeO_3$ crystals in the grown ZnSe film and their gradual crystalline improvement upon annealing play a crucial role in influencing the optical absorption and the photosensitivity of the ZnSe film via photo-carrier generation and absorption processes. A comparative analysis of the photosensitivity of ZnSe samples with that of the CdS thin film, chosen as a model semiconductor, further establishes the significance of $ZnSeO_3$ in controlling the photosensitivity of the ZnSe film.

ACKNOWLEDGMENTS

The authors acknowledge the Department of Physics, University of Calcutta, for extending XRD measurement facilities. One of the authors (B.K.) gratefully acknowledges the University Grant Commission, New Delhi, for awarding the UGC-MANF fellowship.

[1]M. A. Haase, J. Qiu, J. M. DePuydt, and H. Cheng, Appl. Phys. Lett. **59**, 1272 (1991).
[2]H. Morkoç, S. Strite, G. B. Gao, M. E. Lin, B. Sverdlov, and M. Burns, J. Appl. Phys. **76**, 1363 (1994).
[3]K. Katayama, H. Matsubara, F. Nakanishi, T. Nakamura, H. Doi, A. Saegusa, T. Mitsui, T. Matsuoka, M. Irikura, T. Takebe, S. Nishine, and T. Shirakawa, J. Cryst. Growth **214–215**, 1064 (2000).
[4]F. Engelhardt, L. Bornemann, M. Ko, È. Ntges, T. Meyer, J. Parisi, E. Pschorr-Schoberer, B. Hahn, W. Gebhardt, W. Riedl, and U. Rau, Prog. Photovoltaics **7**, 423 (1999).
[5]S. Yan, S. C. Rai, Z. Zheng, F. Alqarni, M. Bhatt, M. A. Retana, and W. Zhou, Adv. Electron. Mater. **2**, 1600242 (2016).
[6]X. Fang, S. Xiong, T. Zhai, Y. Bando, M. Liao, U. K. Gautam, Y. Koide, X. Zhang, Y. Qian, and D. Golberg, Adv. Mater. **21**, 5016 (2009).
[7]P. Chattopadhyay, B. Karim, and S. Guha Roy, J. Appl. Phys. **114**, 243506 (2013).
[8]G. Bakiyaraj and R. Dhanasekaran, Appl. Nanosci. **3**, 125 (2013).
[9]K. G. Rao, K. V. Bangera, and G. K. Shivakumar, Solid State Sci. **13**, 1921 (2011).
[10]C. M. Collier and J. F. Holzman, Appl. Phys. Lett. **104**, 042101 (2014).
[11]J. Sharma, H. Singh, and T. Singh, J. Sci.: Adv. Mater. Devices **2**, 432 (2017).
[12]J. Sharma, H. Singh, T. Singh, and A. Thakur, J. Mater. Sci.: Mater. Electron. **29**, 5688 (2018).
[13]R. L. Petritz, Phys. Rev. **104**, 1508 (1956).
[14]A. E. Rakhshani, J. Phys.: Condens. Matter **12**, 4391 (2000).
[15]F. Urbach, Phys. Rev. **92**, 1324 (1953).
[16]M. Ganchev, N. Stratieva, E. Tzvetkova, and I. Gadjov, J. Mater. Sci.: Mater. Electron. **14**, 847 (2003).
[17]A. Kathalingam, T. Mahalingam, and C. Sanjeeviraja, Mater. Chem. Phys. **106**, 215 (2007).
[18]G. M. Lohar, S. K. Shinde, and V. J. Fulari, J. Semicond. **35**(11), 113001 (2014).
[19]Z. K. Heiba and K. El-Sayed, Egypt. J. Solids **23**, 37 (2000).
[20]Z. K. Heiba, Powder Diffr. **17**, 191 (2002).
[21]M. Verma, A. Kaswan, D. Patidar, K. B. Sharma, and N. S. Saxena, J. Mater. Sci.: Mater. Electron. **27**, 8871 (2016).
[22]K. Yadav, Y. Dwivedi, and N. Jaggi, J. Mater. Sci.: Mater. Electron. **26**, 2198 (2015).
[23]R. B. Kale and C. D. Lokhande, Appl. Surf. Sci. **252**, 929 (2005).
[24]E. L. Khlopochkina, P. E. Gaivoronskii, E. M. Gavrishchuk, Y. E. Elliev, and E. V. Yashina, Russ. J. Appl. Chem. **74**, 1079 (2001).
[25]A. M. Chaparro, C. Maffiotte, J. Herrero, and M. T. Gutierrez, Surf. Interface Anal. **30**, 522 (2000).
[26]A. M. Chaparro, C. Maffiotte, M. T. Gutierrez, and J. Herrero, Thin Solid Films **358**, 22 (2000).
[27]S. Kolhe, S. K. Kulkarni, A. S. Nigavekar, and S. K. Sharma, Sol. Energy Mater. **10**, 47 (1984).
[28]P. K. Nair, O. G. Daza, A. A. Readigos, J. Campos, and M. T. S. Nair, Semicond. Sci. Technol. **16**, 651 (2001).
[29]P. K. Nair, M. T. S. Nair, J. Campos, and L. E. Sansores, Sol. Cells **22**, 211 (1987).
[30]M. T. S. Nair, P. K. Nair, and J. Campos, Thin Solid Films **161**, 21 (1988).
[31]P. K. Nair, J. Campos, and M. T. S. Nair, Semicond. Sci. Technol. **3**, 134 (1988).
[32]A. E. Rakhshani and A. S. Al-Azab, J. Phys.: Condens. Matter **12**, 8745 (2000).